Roles of resonances and recollisions in strong-field atomic phenomena. II. High-order harmonic generation

Richard Taïeb, Valérie Véniard, Joseph Wassaf, and Alfred Maquet
Laboratoire de Chimie Physique-Matière et Rayonnement, Université Pierre et Marie Curie, 11, Rue Pierre et Marie Curie 75231, Paris Cedex 05, France

(Received 9 April 2003; published 11 September 2003)

The theoretical developments presented in a preceding companion paper by Wassaf *et al.* [Phys. Rev. A **67**, 053405 (2003)], for simulating photoelectron spectra, are used to address several issues regarding the harmonic generation process. Both above-threshold Ionization (ATI) and high-order harmonic generation are observed when atoms are submitted to a laser field with intensity around $I=10^{14}$ W cm^{-2}. Here, we demonstrate that the resonances, together with multiple recollisions processes, which have been shown to be at the origin of enhancements of the magnitudes of ATI peaks in the high-energy range, can also play a determining role on the magnitudes of harmonic lines within the plateau. These findings have been obtained via a set of quantum and classical simulations for two classes of one-dimensional model potentials, i.e., either long range (Coulomb-like) or short range (with an exponentially decreasing tail). They are confirmed by following the time evolution of the emission rate of selected harmonics with the help of a (waveletlike) Gabor time-frequency analysis.

DOI: 10.1103/PhysRevA.68.033403 PACS number(s): 32.80.Rm, 42.65.Ky

I. INTRODUCTION

A companion paper, hereafter referred to as I [1], is dedicated to the theoretical study of conspicuous enhancements seen in the plateaus located in the high-energy range in above-threshold ionization (ATI) spectra. There, we have evidenced the important role of resonances and of the multiple recollision mechanism in the physics of this process. The motivation of the present paper is to investigate if similar enhancements could be observed in high-order harmonic generation (HHG) spectra.

High-order harmonics of the fundamental frequency are generated when atoms are irradiated by a strong laser field. This highly nonlinear process has motivated a considerable interest from both the points of view of fundamental physics and of possible application [2]. The main reason for this interest comes from the fact that harmonic spectra exhibit a remarkable plateau that can range from the uv to the soft x-ray domain (for two very recent accounts of the advances in the field, see Refs. [3,4]). In short, harmonics are a promising source of intense and coherent high-frequency radiation, with pulse durations in the femtosecond and even attosecond ranges [5].

Sizable conversion yields from a strong laser pulse to HHG emission from atoms, in the range 10^{-6}–10^{-5}, have been recently achieved at laser intensities around $I \approx 10^{14}$–10^{15} W cm^{-2}. At these intensities, it is known that ATI takes place also with significant probability. In fact, HHG and ATI are two competing processes, the main reason is the depletion of the ground-state population as ionization proceeds. This leads to a decrease in time of the harmonic emission yield during the laser pulse. Furthermore, the competition also arises from the two alternative choices when the electron recollides with the nucleus. Moreover, at the macroscopic level, the transformation of the atom sample, progressively becoming a plasma, modifies the phase-matching properties of the emitting medium. Ionization, at the microscopic and macroscopic levels, contributes to lower the overall emission yield from the sample. It is thus of interest to investigate simultaneously the dynamics of ATI (paper I) and HHG (present work) in the same systems.

It turns out that the physics of the two processes shares many common features. First, from the simple phenomenological point of view, both ATI and HHG exhibit remarkable plateaus in the high-energy domain of their respective spectra [6]. As emphasized in I, it is recognized that the range of these plateaus is linked to the instantaneous kinetic energy of the laser-driven electrons, when they recollide with the nucleus. In this context, a convenient yardstick for measuring the electron energy is the ponderomotive energy: $U_p = q^2F_0^2/(4m\omega^2)$ that corresponds to the averaged kinetic energy of a free electron embedded within a field with amplitude F_0 and frequency ω. It is proportional to the laser intensity: $I_L = \frac{1}{2}\sqrt{(\epsilon_0/\mu_0)}|F_0|^2$. It has been shown that, in ATI spectra, the photoelectrons with kinetic energies $E_{kin} \geqslant 2U_p$ have experienced at least one recollision with their parent ionic core [7]; see also I and references therein. Similarly, in HHG emission spectra, the width of the first plateau goes up to a maximum energy $\omega_{max} \approx I_p + 3.2U_p$, where I_p is the ionization energy of the atom considered [8]. Here, the quantity $3.2U_p$ coincides with the maximum instantaneous kinetic energy that can be acquired by an electron coming back to the origin after having been ejected, via tunneling, from the atom.

We note that, inherent to the above picture, is the idea that the electron is primarily promoted in the continuum via tunneling, i.e., with zero initial velocity. However, under special conditions, a fraction of the electrons can be ejected from excited states located *above* the barrier formed by the combination of the atomic potential and of the laser field, i.e., with nonzero initial velocities. Among these electrons, some of them can recollide several times with the ionic core. As shown in I, this can have important consequences on the shape of the plateaus in ATI spectra. An objective of the

present work is to study the possible influence of such processes on the harmonic emission yields. To this end, we have performed a set of simulations and analysis, paying special attention to the roles of resonances and multiple recollisions.

Regarding the resonances, we mention that the question of their importance has been addressed since the early theoretical studies on HHG. For instance, they play a dominant part in calculations based on two-level model systems [9–12]. In multilevel atoms, the role of resonances and the interplay between the contributions of bound states and of the continuum has motivated several studies [13,14]. Interestingly, resonances at the Kepler frequencies and their multiples dominate also the dynamics of the driven dipole in classical hydrogen atoms [15–17]. The problem has been revisited more recently by solving the time dependent Schrödinger equation (TDSE) for more realistic atomic model potentials [18–20]. And the question of the possible connection with channel closings has been addressed for model potentials, either zero range [21–23], or long and short range [24]. In all these simulations it has been found that, under resonant conditions, significant enhancements of the harmonic emission yields are observed. This has been confirmed in the experiments performed by Toma *et al.* [25].

However, it turns out that the enhancements found in the simulations are not limited to the harmonic order associated to the multiphoton resonance. *R*-matrix Floquet calculations [20] provide an interesting example of this point; in Ar, for a three-photon resonance not only the third harmonic is enhanced, but also the fifth and seventh. A similar behavior has been evidenced in simulations made for K atoms [18], where it is not only the harmonic associated with the multiphoton resonance that is enhanced.

Here, we have tried to uncover the physical mechanism that could be responsible for this *a priori* unexpected behavior. Guided by our study of ATI in similar conditions, we have investigated the role of multiphoton resonances and of recollisions. As we shall show below, by combining quantum TDSE calculations, supported by a Floquet analysis and classical trajectory simulations, one has evidenced the important role of the trajectories that can revisit the origin several times. Further insights in the time dependence of the dynamics has been obtained from a time-frequency (waveletlike) analysis of the atomic dipole [26,27]. We mention that all our simulations are performed within a single active electron picture, which is well adapted here, given the laser intensity range considered.

The organization of the paper is as follows. In the following section, we shall briefly present the theoretical background. The results of a set of quantum calculations (TDSE and Floquet) performed for a long-range one-dimensional model potential, are presented in Sec. III. The analysis is supported by classical simulations. The results of a similar set of calculations performed for the case of a short-range potential are analyzed in Sec. IV. The last section is devoted to the comparison of the results we have obtained for the two types of potentials and to a general discussion. In the following, atomic units will be used unless otherwise mentioned.

II. THEORY

Before we introduce the technical details of the calculations, we mention that the main difficulty encountered when analyzing the physical mechanisms at work in this class of processes comes from the fact that at the laser frequency and for the intensity range considered, one is almost exactly at the border between the so-called ''multiphoton'' and ''tunneling'' regimes. A consequence, outlined in a recent analysis of strong-field ionization, is that neither tunneling nor multiphoton ionization dominates the dynamics [28]. An illustration of the interplay between the two regimes is that the envelope of the ATI peaks can be modeled via semiclassical arguments (implying that the electrons are released in the continuum via tunneling), while the multicomponent structure of each ATI peak is the signature of resonant multiphoton transitions involving atomic excited states [29]. In fact, in I, it has been shown that ATI spectra are made of two classes of photoelectrons: many of them are ejected via tunneling, while the ones with energies where enhancements take place have experienced a multiphoton resonant transition towards an excited state, prior to being ionized. This strongly suggests that, to describe the mechanisms at work in this class of processes, it is necessary to rely on both the quantal and classical approaches, in order to encompass the different aspects of the dynamics, see, for instance, Ref. [30].

Here, the quantum calculations have been performed by solving the TDSE for one-dimensional potentials modeling the single-electron atomic response to a linearly polarized laser pulse. We have considered two distinct cases:

(i) The ''soft-Coulomb'' potential [31]

$$V(x) = -\frac{1}{\sqrt{c+x^2}}, \tag{1}$$

which behaves asymptotically as a one-dimensional Coulomb potential. Here, we have chosen the same value of the parameter $c=1.41$, as in I: the ground-state energy corresponds to the one of Ar atoms, i.e., $E_0=-0.58$ a.u.

(ii) The short-range Pöschl-Teller potential [32] is of the general form

$$V_{P-T}(x) = -\frac{a}{ch^2(\alpha x)}, \tag{2}$$

where the choice of parameters a and α determines the ground-state energy and the number of bound states. Here, for $a=0.828$ and $\alpha=0.978$, there is only one bound state with energy $E_0=-0.3938$ a.u., i.e., the same as in I.

HHG spectra are deduced from the power spectrum of the acceleration of the time-dependent atomic dipole,

$$a(t) = \left\langle \Psi(t) \left| -\frac{\partial V(x)}{\partial x} \right| \Psi(t) \right\rangle, \tag{3}$$

obtained by solving the TDSE:

$$i\frac{\partial}{\partial t}\Psi(x,t) = \left[H_0 + i\frac{A(t)}{c}\frac{\partial}{\partial x} \right]\Psi(x,t), \tag{4}$$

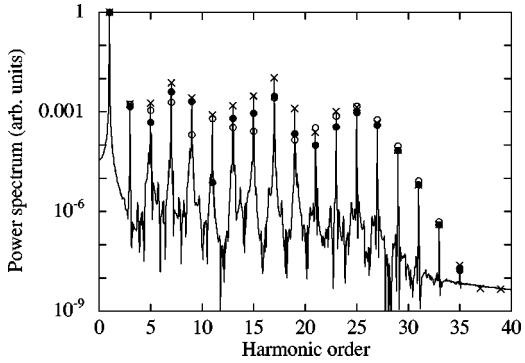

FIG. 1. Normalized high-order harmonic spectra for the long-range potential, Eq. (1), for $\omega=0.0577$ a.u. and a pulse duration of 34 cycles. Open circles, crosses, and full circles correspond to intensities of 1.137×10^{14} W cm^{-2}, $I_{n=6}=1.145\times10^{14}$ W cm^{-2}, and 1.152×10^{14} W cm^{-2}, respectively.

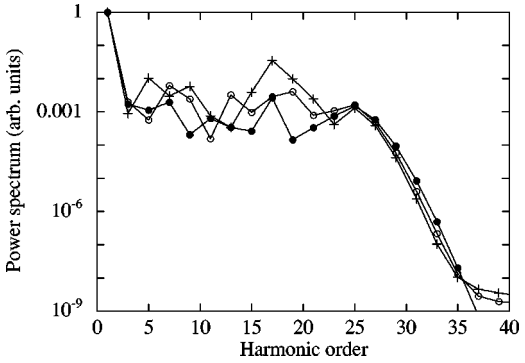

FIG. 2. Normalized high-order harmonic spectra for the long-range potential, Eq. (1), for $\omega=0.0577$ a.u., a pulse duration of 34 cycles, and at intensities around the $n=3$ resonance. Open circles, crosses, and full circles correspond to intensities of 1.10×10^{14} W cm^{-2}, $I_{n=3}=1.12\times10^{14}$ W cm^{-2}, and 1.14×10^{14} W cm^{-2}, respectively.

where $A(t)$ is the vector potential of the field and

$$H_0=-\frac{1}{2}\frac{\partial^2}{\partial x^2}+V(x). \tag{5}$$

We note that the term proportional to the field strength $F(t)=-(1/c)(\partial A(t)/\partial t)$ has been omitted in the expression of the dipole acceleration. Its inclusion would contribute to modify only the component at ω in the power spectra. In our simulations, the magnitude of this line is thus directly linked to the elastic (Rayleigh-) scattering yield. Accordingly, in order to perform meaningful comparisons between harmonic emission rates at different laser field strengths, we have normalized the spectra to the height of the first line at ω.

The numerical resolution of the TDSE and the Floquet calculations rely on the techniques described in I. We have also used the same type of classical trajectory simulations. Power spectra of the time-dependent dipole are deduced from standard Fourier analysis. In addition, we have investigated the time dependence of the emission rate of selected harmonics via a time-frequency (Gabor) analysis [26,27], see below.

III. HARMONIC GENERATION FROM A LONG-RANGE POTENTIAL

Shown in Fig. 1, are examples of HHG spectra, simulated when a system described by the ''soft-Coulomb'' potential, Eq. (1), is submitted to a trapezoidal laser pulse with frequency $\omega=0.0577$ a.u.≈1.57 eV, with a total duration of 34 cycle including one-cycle turn-on and turn-off. The chosen intensities are representative of the range around the value ($I_{n=6}=1.145\times10^{14}$ W cm^{-2}) at which an enhancement is observed in the high-energy part of the ATI spectrum for the same system, see Ref. [1]. There, through Floquet calculations, it has been shown that at this intensity, there is a 14-photon resonance resulting from a (avoided) crossing between the ground state and the $n=6$ ''dressed'' states supported by the potential, Eq. (1). As seen in the figure, there are significant enhancements of the (scaled-) emission yields, in the range $H7$-$H19$, where HN represents the Nth harmonic. Outside this range, the scaled magnitudes are not changed significantly.

As shown in Fig. 2, a similar behavior is observed at intensities close to $I_{n=3}=1.12\times10^{14}$ W cm^{-2}, at which there is a 13-photon resonance with the state $n=3$. Here also, several harmonic lines are enhanced between $H5$ and $H21$, with the notable exception of $H13$ itself. We note, however, that the vicinity of the resonance on the state $n=6$ at $I_{n=6}=1.145\times10^{14}$ W cm^{-2} complicates the analysis of the spectrum at 1.12×10^{14} W cm^{-2}.

In order to uncover the physical mechanisms that give rise to these enhancements, we have considered first the case of the multiphoton resonance, which takes place at $I_{n=6}=1.145\times10^{14}$ W cm^{-2}, involving a 14-photon transition. As mentioned in the Introduction, it is expected that the (scaled) magnitudes of neighboring harmonics, i.e., $H13$ and $H15$, could be enhanced. However, several other harmonics (from $H7$ to $H19$) are also enhanced, precisely at this intensity. In I, it has been shown that the combination of the resonance *and* of the existence of classical trajectories revisiting the origin periodically, is a necessary condition for observing the enhancements in the plateau region of ATI spectra. Here, we shall investigate how the same processes influence the harmonic spectra.

A first assessment of the importance of the periodic trajectories is evidenced in Fig. 3, where we have illustrated the influence of the pulse length on the spectra. There, we have compared the harmonic yields, for two different pulse durations for (i) the resonant intensity [Fig. 3(a)] and (ii) another neighboring (nonresonant) intensity [Fig. 3(b)]. In the latter case, the two spectra, computed for 18- and 34-cycle pulse durations, coincide almost exactly, when scaled as explained above. The small differences are likely to be ascribed to the interplay with ionization that depletes more significantly the ground state population when the pulse is longer. This contrasts markedly with the case of the resonant intensity $I_{n=6}$: there [Fig. 3(a)], the longer the pulse, the larger the (scaled) magnitudes of the lines in the range $H7$–$H19$.

The explanation for this behavior lies in the existence of a class of trajectories that can revisit the origin many times,

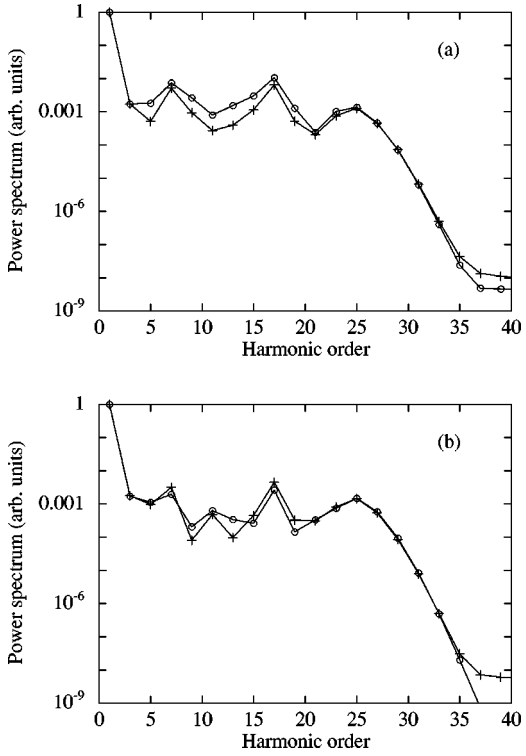

FIG. 3. Comparison of the (scaled-) harmonic emission yields, at $\omega=0.0577$ a.u., for two different pulse durations: crosses correspond to 18-cycle and open circles to 34-cycle durations. (a) Resonant intensity $I_{n=6}=1.145\times10^{14}$ W cm^{-2} with the $n=6$ state, see text; (b) nonresonant intensity 1.137×10^{14} W cm^{-2}.

twice per laser cycle, after the electrons have been ejected from the state $n=6$. Each time an electron recollides, it can either (i) be rescattered elastically, thus being available for subsequent recollisions, twice per laser cycle; (ii) be ionized, thus contributing to the high-energy part of the ATI spectrum; or, (iii) recombine with the core, thus emitting harmonic radiation.

New electrons that follow these trajectories are ejected twice per laser cycle which entails that, given the relatively low probabilities for ionization or recombination, the population available for harmonic emission is growing in time. This leads to the prediction that, for the corresponding harmonics, the emission rate should *increase* during the pulse.

The case of one of these trajectories had been considered, for the sake of illustration, in I (see Ref. [1], Fig. 7). There, it had been observed that the instantaneous kinetic energy of the electron when it returns to the origin, $E_{kin}(x=0)$, is comprised within the range $1.4U_p\leqslant E_{kin}(x=0)\leqslant 2U_p$. We note that in the conditions considered here, one has $U_p\approx 4.26\omega$. Those electrons, which, in the course of the recollision recombine in the ground state $n=0$, generate harmonics with energies $\omega_H\approx E_{kin}(x=0)+I_p|_{n=0}$, i.e., that are comprised in the range $15.9\omega\leqslant\omega_H\leqslant 18.5\omega$. This can certainly account for the enhancement in the emission spectrum at $\omega_H=17\omega$, see Fig. 1.

However, there is also the possibility that the electrons following the same trajectories recombine in the state $n=6$ from which they originate. Then, they would generate harmonics with energies $\omega_H\approx E_{kin}(x=0)+I_p|_{n=6}$. Translated in the laser frequency scale, one has $7\omega\leqslant\omega_H\leqslant 9\omega$, a result which accounts for the observed enhancements of the harmonics $H7$ and $H9$, see Fig. 1. These results have been obtained for one particular trajectory [labeled (A) in Fig. 6(b) in I] that revisits the origin a large number of times. In fact, the analysis of the classical trajectories indicates that there is a class of such trajectories that reencounter the origin with slightly different instantaneous kinetic energies. This explains why, under resonant conditions, the enhancements observed in the simulations span a quite large number of harmonics and are not limited to the resonant frequency and its immediate neighbors.

Another way to assess the importance of the multiple recollisions is to follow in time the variations of the normalized emission rates of the harmonic lines. This can be done with the help of a time-frequency (waveletlike) analysis of the dipole acceleration $a(t)$, Eq. (3).

To this end, we have used a ''windowed'' version of the Fourier transform, which allows to scan the time domain by translating the window, with suitable width, in order to follow the time variations of the frequency content of the dipole acceleration signal. Here, we have chosen to use the Gabor transform that optimizes the choice of the size of the window in accordance with the uncertainty principle. More precisely, the window is a Gaussian function:

$$g_\alpha(t)=\frac{1}{2\sqrt{\pi\alpha}}e^{-(t^2/4\alpha)}, \tag{6}$$

and the Gabor transform of the dipole acceleration $a(t)$ is

$$(\mathcal{G}_t^\alpha a)(\omega)=\int_{-\infty}^{+\infty}[e^{-i\omega t'}a(t')]g_\alpha(t'-t)dt'. \tag{7}$$

We mention that similar techniques have been used already in the context of studies of the time dependence of the harmonic emission. Earlier studies have been reported in Refs. [26,27] and recent references include Refs. [13,19,35,36]. Here, we have followed the time dependence of the Gabor transform components associated to the harmonic frequencies at different intensities. As the Gabor transform decomposes exactly the Fourier transform of a signal, the variations in time of a given harmonic frequency component provide a direct measure of the variations of the corresponding time-dependent emission rate. A typical example is shown in the Fig. 4. There, the time dependences of the harmonic frequency components $H5$–$H25$ are reported for 34-cycle trapezoidal pulses at the resonant intensity $I_{n=6}$ [Fig. 4(a)] and at a neighbor non-resonant intensity 1.137×10^{14} W cm^{-2}, [Fig. 4(b)]. The parameter α, which governs both the time and frequency resolution according to the uncertainty principle, has been chosen as $\alpha=33.3/\omega_L^2$. The time dependence is shown after five laser cycles, so that the contributions of the transients generated during the one-cycle turn-on have died out [the corresponding Fourier transformed power spectra, computed in the same conditions, have been presented in Figs. 3(a) and 3(b)]. At resonance, two harmonic components are dominant, with emission rates

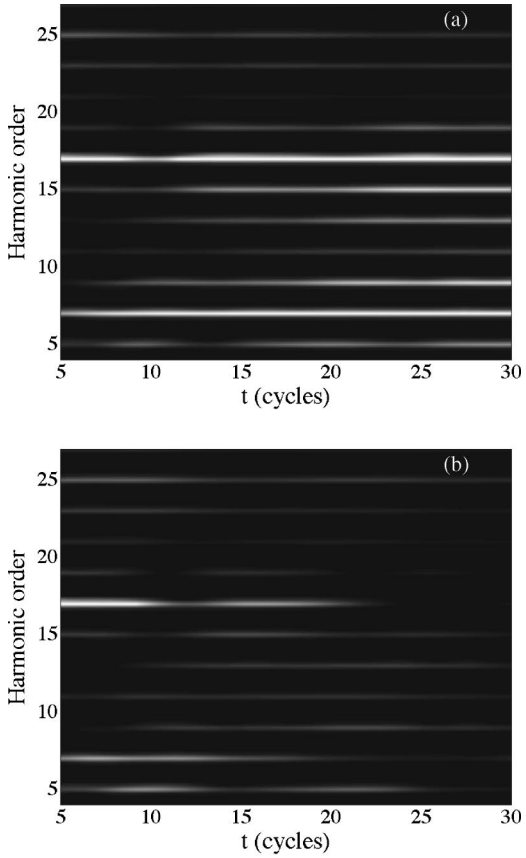

FIG. 4. Time dependence of the Gabor transform components of the dipole acceleration for the long-range potential, Eq. (1), with $\omega=0.0577$ a.u. and a 34-cycle trapezoidal pulse (see text). (a) Resonant intensity $I_{n=6}=1.145\times10^{14}$ W cm^{-2}; (b) nonresonant intensity 1.137×10^{14} W cm^{-2}.

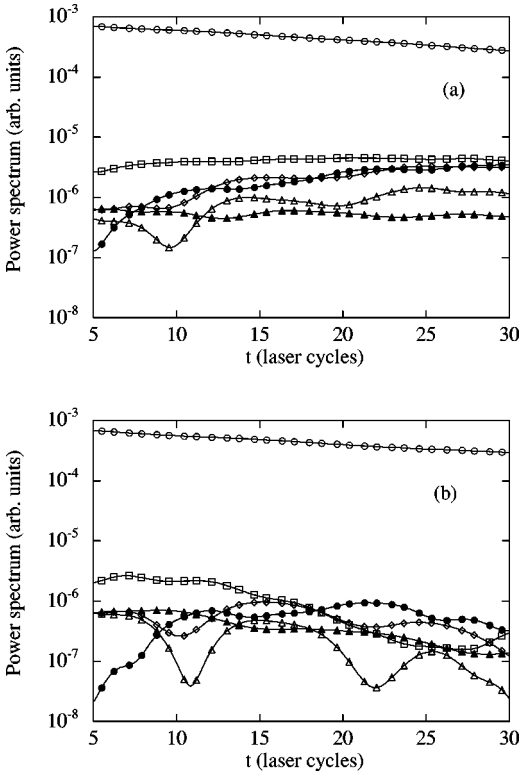

FIG. 5. Time dependence of the Gabor transform components of the dipole acceleration at selected harmonic frequencies and at the Rayleigh $H1=\omega=0.0577$ a.u. driving frequency. Open circles, open squares, filled circles, diamonds, and open and filled triangles correspond to $H1$, $H7$, $H9$, $H15$, $H19$, and $H23$, respectively. Same conditions as in Figs. 4. (a) Resonant intensity $I_{n=6}=1.145\times10^{14}$ W cm^{-2}; (b) nonresonant intensity 1.137×10^{14} W cm^{-2}.

that do not decline with time: (i) $H17$, which can be associated to the periodic trajectories that emerge from the resonant $n=6$ state and recombine subsequently in the ground state; and (ii) $H7$, which can be associated to periodic trajectories that emerge from the resonant $n=6$ state and recombine subsequently in the same state, see the above discussion.

Under such resonant conditions, one observes that the emission rates for these harmonics and also for the neighboring ones, continue to grow in time. This represents a clear signature of the existence of periodic trajectories that experience many recollisions with the ionic core: The longer the pulse, the higher is the probability for recombining with harmonic emission, see I for a similar discussion regarding ATI spectra. We note that this holds so long as the overall ionization yields remain relatively small, so that the depletion of the ground-state population is not significant.

The evolution is much different in nonresonant conditions, as shown in Fig. 4b. Then, one observes that, in general, the harmonic emission rates decrease in time. This trend is expected, on the grounds of the general picture that suggests that, as ionization proceeds, the depletion of the bound-state population hinders harmonic emission yields.

This is confirmed on closer inspection, when recording the time dependence of selected harmonic frequency components, as shown in Figs. 5(a) and 5(b), for the same conditions as in Figs. 4(a) and 4(b). For the sake of comparison, we have also shown the time evolution of the emission rate for the Rayleigh component $H1$ at ω. As the Rayleigh-scattering rate is directly proportional to the bound-state population, it steadily decreases with time, as expected. By contrast, at the resonant intensity $I_{n=6}$, Fig. 5(a), one observes that the emission rates of $H7$ and $H17$, as well as some of their neighbors, *grow* with time. As shown in Fig. 5(b), the trend is most different at a nonresonant intensity. There, besides occasional fluctuations, the variations are characterized by a decrease, globally parallel to the decline of the Rayleigh $H1$ component.

However, the emission rates of $H9$ and $H11$ behave differently. They seem to grow in time like in the resonant case. This can be explained because of the presence, even in the nonresonant case, of quasiperiodic trajectories that are born near the maximum of the electric field, via tunneling. These trajectories return many times close to the origin with almost zero kinetic energy. Therefore the harmonics emitted by this class of trajectories would be around $I_p\approx10\omega$, in agreement with the observed behavior of $H9$ and $H11$.

We stress that, between Figs. 4(a) and 4(b), on the one hand and 5(a) and 5(b) on the other hand, the field intensities differ only by 0.6%. The important differences observed between the corresponding rates are a clear signature of a resonance phenomenon.

To summarize the results presented in this section, we have confirmed that, in a long-range model potential, multiphoton resonances on excited states give rise to significant enhancements of several harmonic lines. The mechanism invoked for explaining how these short-lived states can play such an important role in the dynamics of harmonic emission, singles out the essential role of the electron trajectories that can recollide many times with the ionic core, twice per laser cycle, see Ref. [1]. In resonant conditions, the driven electron can recombine either in the ground state or in the intermediate (resonant) state from which it was ejected. This feature accounts for the range of harmonics that are enhanced.

We mention also that we have not found similar enhancements at intensities associated with channel closings for the long-range potential we used. Concerning this latter point, there is an ongoing discussion dedicated to the question of the role of channel closings in harmonic spectra. We shall address this question in the following section.

IV. HARMONIC GENERATION FROM A SHORT-RANGE POTENTIAL: EMISSION DYNAMICS IN THE ABSENCE OF EXCITED STATES

Several studies performed for a zero-range δ-function potential, via a *S*-matrix formalism, have concluded to the existence of enhancements in HHG spectra at intensities close to those corresponding to channel closings Refs. [21–23], see also Ref. [24]. These studies are continuations of similar calculations performed for simulating ATI spectra, where enhancements were also found in the same conditions [21,37–40]. As our above simulations, performed for a long-range potential, do not reproduce such a behavior, we have investigated the physical reasons at the origin of these differences.

To this end, we have solved the TDSE for the case of a short-range Pöschl-Teller potential, Eq. (2), which does not support any excited state. Harmonic spectra have been simulated as explained above, for the same set of parameters as in I. As no resonant mechanism involving an excited state can be invoked in these conditions, we have first explored the possible role of the channel closings. The corresponding intensities have been determined with the help of the Floquet analysis described in I, Sec. III B [1]. In the relevant intensity range, where ATI and HHG yields are significant, 10- and 11-photon channel closings take place at the following intensities: $I_{10}\approx 8.37\times 10^{13}\ \mathrm{W\,cm^{-2}}$ and $I_{11}\approx 1.105\times 10^{14}\ \mathrm{W\,cm^{-2}}$, respectively. We note that these intensities are derived from the Floquet analysis and that they differ slightly from the approximate values: $N\omega\approx|\epsilon_0|+U_p$, where ϵ_0 is the ground-state energy.

The results of our simulations for the scaled emission yields at intensities around I_{10}, i.e., at the 10-photon channel closing, are shown in Fig. 6. When the intensity is scanned across the threshold, it can be checked that the changes in the magnitudes of the HHG lines are much less pronounced than in the vicinity of a resonance in the soft-Coulomb case. We mention that an enhancement was found in the high-energy part of the ATI spectrum, close to this intensity, see Ref. [1]. We have also searched the intensity range around I_{11}, without finding any significant enhancement of the harmonic yields. We note that recent simulations, based on TDSE calculations for a class of short-range potentials with a finite number of states, indicate also that there is no clear indication of a threshold effect [24]. Here, we confirm these findings in the case of a system with no excited state.

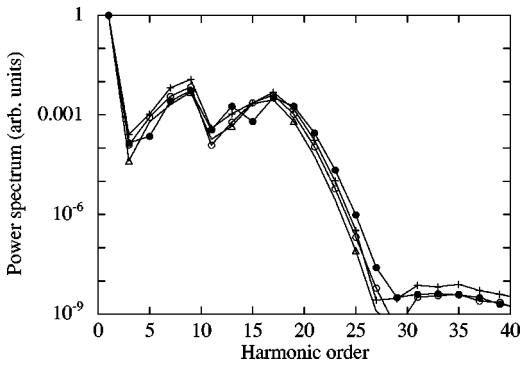

FIG. 6. Normalized high-order harmonic spectra for the short-range Pöschl-Teller potential, Eq. (2), at intensities around $I_{10}\approx 8.37\times 10^{13}\ \mathrm{W\,cm^{-2}}$, where the 10-photon channel closing takes place. The other field parameters are the same as in Fig. 1. Triangles, open circles, crosses, and full circles correspond to intensities of $7.90\times 10^{13}\ \mathrm{W\,cm^{-2}}$, $8.17\times 10^{13}\ \mathrm{W\,cm^{-2}}$, $I_{10}=8.37\times 10^{13}\ \mathrm{W\,cm^{-2}}$, and $8.75\times 10^{13}\ \mathrm{W\,cm^{-2}}$, respectively.

Surprisingly, one can find the signature of a resonant behavior for this system, at intensities around $I_{crit}\approx 9.46\times 10^{13}\ \mathrm{W\,cm^{-2}}$, i.e., far from any channel closing, see Fig. 7. In fact, in the same conditions, a high-energy enhancement was found in the ATI spectrum, see Fig. 11 in I [1]. There, it was shown that at the same intensity a crossing occurs between the ground state and a laser-induced state (LIS) [41,42]. More precisely, the LIS labeled (A) in Fig. 13 in I [1] can be populated via a 10-photon transition from the ground state. This confirms our previous findings that a LIS can play the same role as an excited state in a resonant multiphoton process.

Again, the electrons ejected from this state located above

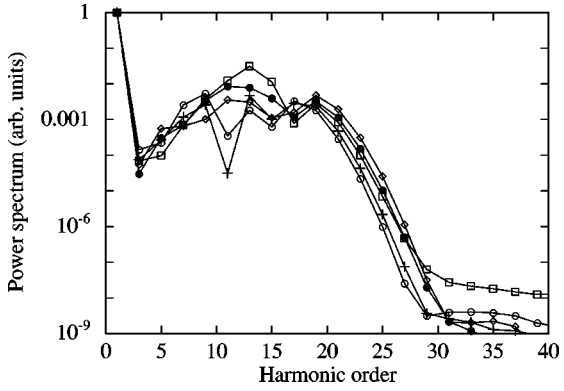

FIG. 7. Normalized high-order harmonic spectra for the short-range potential, Eq. (2), for intensities close to the resonance with a LIS, see text. Open circles, crosses, squares, full circles, and diamonds correspond to intensities of $8.75\times 10^{13}\ \mathrm{W\,cm^{-2}}$, $9.10\times 10^{13}\ \mathrm{W\,cm^{-2}}$, $9.46\times 10^{13}\ \mathrm{W\,cm^{-2}}$, $9.83\times 10^{13}\ \mathrm{W\,cm^{-2}}$, and $1.02\times 10^{14}\ \mathrm{W\,cm^{-2}}$, respectively.

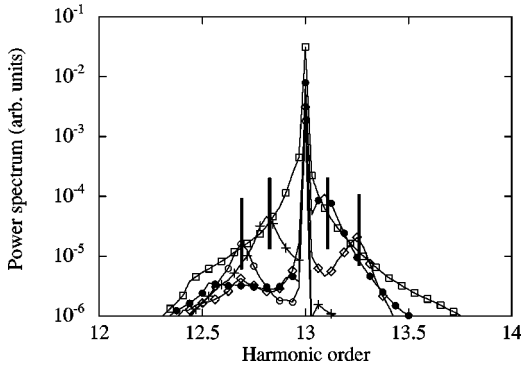

FIG. 8. Normalized high-order harmonic spectra for the short-range potential, Eq. (2), for intensities around the resonance with the LIS (A). Enlargement of Fig. 7 around the 13th harmonic. The positions of the hyper-Raman frequencies are indicated by vertical lines, see text.

the barrier can recollide several times with the nucleus, with a nonzero kinetic energy. If they recombine in the ground state they generate harmonics in the range $H11$–$H15$. As seen in Fig. 7, these harmonics are precisely those which are enhanced at the resonant intensity.

Another way to assess the importance of the role of the LIS is to look into the details of the power spectrum. Indeed, in addition to the harmonic lines, one observes also lines associated to hyper-Raman transitions at frequencies $\Omega_n = \epsilon_A + \epsilon_0 \pm n\omega$, where ϵ_A and ϵ_0 are the energies of the LIS and of the dressed ground state, respectively [33,34]. As these energies are intensity dependent, the position of the line changes as a function of the field intensity. This is illustrated in Fig. 8, where an enlargement of the power spectrum around $H13$ is shown. The frequency of the line can be deduced from the Floquet spectrum shown in Fig. 13 in I [1]. One observes that the magnitude of $H13$ is maximum when the hyper-Raman line merges with the harmonic line, i.e., exactly at resonance. As such a short-range potential model is approximately valid for describing negative ion species, the observation of such enhancements would be the signature of the presence of a LIS, the existence of which is still debated [42].

V. DISCUSSION AND CONCLUSIONS

In this paper, we have addressed the question of the enhancements found in simulations and in an experiment for HHG emission spectra at intensities for which there is a multiphoton resonance with an excited state. Several simulations, based on the resolution of the TDSE for different model potentials, indicate that in addition to the harmonics at frequencies close to the resonant one, there is a notable enhancement of a large number of other harmonics located in the plateau. We have investigated the physical origin of this peculiar behavior.

Our investigations have been based on the resolution of the TDSE for one-dimensional model potentials, either long range (soft-Coulomb) or short range (Pöschl-Teller). The numerical results for harmonic emission yields, as deduced from a TDSE treatment, have been interpreted with the help of a Floquet and of a classical trajectory analysis. The time dependence of the emission rates has been also discussed via a time-frequency (Gabor) analysis of the dipole acceleration.

In the case of a long-range potential, these analyses evidence the essential role of multiphoton resonances involving excited states. This agrees with the results of other simulations [18–20] and experiments [25]. Moreover, our results show that the highly nonlinear dependence of the enhancements on the laser intensity is linked to the existence of oscillating electron trajectories that revisit the origin twice per laser cycle. As they start from the resonantly populated excited state, with a nonzero initial kinetic energy, they still have nonzero instantaneous kinetic energies when they come back to the origin. Then, if they recombine, they can emit harmonic radiation with frequency $\omega_H \approx E_{kin}(x=0) + I_p|_{n=0}$ or $\omega_H \approx E_{kin}(x=0) + I_p|_n$, depending on whether they recombine in the ground state or in the excited state from which they originate. This accounts for the range of the harmonics that are enhanced. Otherwise, the electrons that do not recombine can either contribute to the high-energy part of the ATI spectrum, or be elastically scattered and recollide again. In the latter case, the same scenario repeats. Then, given the relatively low probabilities for ionization or recombination, the population in the laser-driven wave packets increases continouously and the probability for harmonic emission grows with the number of allowed recollisions. This leads to the prediction that the magnitude of the enhancement should increase nonlinearly with the duration of the laser pulse. We believe that this prediction should be amenable to experimental verifications.

Regarding the case of short-range potentials, adapted to the description of the response of negative ions, our analysis shows that LIS can play the same role as excited states in atoms. Accordingly, notable enhancements are found in the simulations of HHG spectra, whenever there is a multiphoton resonance between the ground state and one of these LIS. On the other hand, we have not found a clear indication of a similar resonant behavior at intensities close to the ones associated to ''channel-closings.'' This confirms recent simulations made in short-range potentials supporting only a limited number of excited states, where there was no direct indication of a threshold effect [24]. This contrasts with previous findings, in calculations performed with the help of a (three-dimensional) δ-function potential [21–23].

In conclusion, our results confirm that multiphoton resonances could enhance harmonic emission rates at intensities $\approx 10^{14}$ W cm^{-2} for a Ti:sapphire laser, i.e., at the border between the multiphoton and the tunnelling regime. However, another essential ingredient is the existence of electron trajectories which can experience multiple recollisions with the origin. In our opinion, put together, the resonance and the multiple-recollision mechanisms account for the essential features of resonant harmonic emission in atoms. On the other hand, for short-range model potentials, we have also found that, in some cases, LIS could play the role of excited states in atoms. We believe that this set of results, together with the recent ones on ATI spectra [1], should motivate further investigations in both theory and experiments.

ACKNOWLEDGMENTS

The Laboratoire de Chimie Physique-Matière et Rayonnement is a Unité Mixte de Recherche, Associée au CNRS, UMR 7614, and is Laboratoire de Recherche Correspondant du CEA, Grant No. DSM-98-16. Parts of the computations have been performed at the Centre de Calcul pour la Recherche (CCR, Jussieu, Paris) and at the Institut du Développement et des Ressources en Informatique Scientifique (IDRIS).

[1] J. Wassaf, V. Véniard, R. Taïeb, and A. Maquet, Phys. Rev. A **67**, 053405 (2003); a preliminary account of this work has been published in Phys. Rev. Lett. **90**, 013003 (2003).

[2] Recent reviews include M. Protopapas, C.H. Keitel, and P.L. Knight, Rep. Prog. Phys. **60**, 389 (1997); C.J. Joachain, M. Dörr, and N. Kylstra, Adv. At., Mol., Opt. Phys. **42**, 225 (2000).

[3] S. Kazamias, F. Weihe, D. Douillet, C. Valentin, T. Planchon, S. Sebban, G. Grillon, F. Aug, D. Hulin, and Ph. Balcou, Eur. Phys. J. D **21**, 353 (2002).

[4] A. Paul, R.A. Bartels, R. Tobey, H. Green, S. Weiman, I.P. Christov, M.M. Murnane, H.C. Kapteyn, and S. Backus, Nature (London) **421**, 51 (2003).

[5] Recent references on applications of attosecond pulses from harmonics include A. Baltuska, Th. Udem, M. Uiberacker, M. Hentschel, E. Goulielmakis, Ch. Gohle, R. Holtzwarth, V.S. Yakovlev, A. Scrinzi, T.W. Hansch, and F. Krausz, Nature (London) **421**, 611 (2003); H. Niikura, F. Legaré, R. Hasbani, M. Yu Ivanov, D.M. Villeneuve, and P.B. Corkum, *ibid.* **421**, 826 (2003)

[6] M.D. Perry, A. Szöke, and K.C. Kulander, Phys. Rev. Lett. **63**, 1058 (1989); see also K.J. Schafer, B. Yang, L. F DiMauro, and K.C. Kulander, *ibid.* **70**, 1599 (1993).

[7] G.G. Paulus, W. Becker, W. Nicklich, and H. Walther, J. Phys. B **27**, L703 (1994).

[8] J.L. Krause, K.J. Schafer, and K.C. Kulander, Phys. Rev. Lett. **68**, 3535 (1992); P.B. Corkum, *ibid.* **71**, 1994 (1993).

[9] B. Sundaram and P.W. Milonni, Phys. Rev. A **41**, 6571 (1990).

[10] L. Plaja and L. Roso, J. Mod. Opt. **40**, 793 (1993).

[11] F.I. Gauthey, C.H. Keitel, P.L. Knight, and A. Maquet, Phys. Rev. A **52**, 525 (1995); see also F.I. Gauthey, B.M. Garraway, and P.L. Knight, *ibid.* **56**, 3093 (1997).

[12] A. Di Piazza, E. Fiordilino, and M.H. Mittleman, J. Phys. B **34**, 3655 (2001).

[13] C. Figueira de Morisson Faria, M. Dörr, and W. Sandner, Phys. Rev. A **58**, 2990 (1998).

[14] P.P. Corso, A. Di Piazza, E. Fiordilino, L. Lo Cascio, and F. Persico, J. Mod. Opt. **48**, 1373 (2001).

[15] G. Bandarage, A. Maquet, and J. Cooper, Phys. Rev. A **41**, 1744 (1990); G. Bandarage, A. Maquet, T. Ménis, R. Taïeb, V. Véniard, and J. Cooper, *ibid.* **46**, 380 (1992).

[16] Shih-I Chu, K. Wang, and E. Layton, J. Opt. Soc. Am. **7**, 425 (1990).

[17] J.G. Leopold and D. Richards, J. Phys. B **26**, 1519 (1993).

[18] M.B. Gaarde and K.J. Schafer, Phys. Rev. A **64**, 013820 (2001).

[19] Xi Chu, Shih-I Chu, and C. Laughlin, Phys. Rev. A **64**, 013406 (2001).

[20] M. Plummer and C.J. Noble, J. Phys. B **35**, L51 (2002).

[21] R. Kopold, W. Becker, M. Kleber, and G.G. Paulus, J. Phys. B **35**, 217 (2002).

[22] B. Borca, A.F. Starace, A.V. Flegel, M.V. Frolov, and N.L. Manakov, Phys. Rev. A **65**, 051402(R) (2002).

[23] D.B. Milošević and W. Becker, Phys. Rev. A **66**, 063417 (2002).

[24] C. Figueira de Morisson Faria, R. Kopold, W. Becker, and J.M. Rost, Phys. Rev. A **65**, 023404 (2002).

[25] E.S. Toma, P. Antoine, A. de Bohan, and H.G. Muller, J. Phys. B **32**, 5843 (1999).

[26] P. Antoine, B. Piraux, and Alfred Maquet, Phys. Rev. A **51**, R1750 (1995).

[27] R. Taïeb, A. Maquet, P. Antoine, and B. Piraux, in *Super-Intense Laser-Atom Physics IV*, Vol. 3/13 of *NATO Advanced Studies Institute*, edited by H. G. Muller and M. V. Fedorov (Kluwer, Dordrecht, 1996), p. 445.

[28] A. de Bohan, B. Piraux, L. Ponce, R. Taïeb, V. Véniard, and A. Maquet, Phys. Rev. Lett. **89**, 113002 (2002).

[29] R. Freeman, P.H. Bucksbaum, H. Milchberg, S. Darack, D. Schumacher, and M.E. Geusic, Phys. Rev. Lett. **59**, 1092 (1987).

[30] W. Becker, F. Grasbon, R. Kopold, D.B. Milosevic, G.G. Paulus, and H. Walther, Adv. At., Mol., Opt. Phys. **48**, 35 (2002).

[31] Q. Su and J.H. Eberly, Phys. Rev. A **44**, 5997 (1991).

[32] S. Flügge, *Practical Quantum Mechanics* (Springer, Berlin, 1971).

[33] T. Millack and A. Maquet, J. Mod. Opt. **40**, 2161 (1993).

[34] For a recent discussion on the properties of hyper-Raman scattered light spectra, see M.L. Pons, R. Taïeb, and A. Maquet, Phys. Rev. A **54**, 3634 (1996); see also Ref. [35].

[35] A. Di Piazza and E. Fiordilino, Phys. Rev. A **64**, 013802 (2001).

[36] R. Daniele, F. Morales, A. Di Piazza, and E. Fiordilino, Laser Phys. **11**, 205 (2001).

[37] G.G. Paulus, F. Grasbon, H. Walther, R. Kopold, and W. Becker, Phys. Rev. A **64**, 021401(R) (2001).

[38] A. Lohr, M. Kleber, R. Kopold, and W. Becker, Phys. Rev. A **55**, R4003 (1997); D.B. Milošević and F. Ehlotzky, *ibid.* **58**, 3124 (1998); S.P. Goreslavskiĭ and S.V. Popruzhenko, JETP **90**, 778 (2000).

[39] B. Borca, M.V. Frolov, N.L. Manakov, and A.F. Starace, Phys. Rev. Lett. **88**, 193001 (2002).

[40] S.V. Popruzhenko, P.A. Korneev, S.P. Goreslavski, and W. Becker, Phys. Rev. Lett. **89**, 023001 (2002).

[41] R. Bhatt, B. Piraux, and K. Burnett, Phys. Rev. A **37**, 98 (1988).

[42] J.C. Wells, I. Simbotin, and M. Gavrila, Phys. Rev. Lett. **80**, 3479 (1998); see also the discussion by P. Schlagheck, K. Hornberger, and A. Buchleitner, *ibid.* **82**, 664 (1999); J.C. Wells, I. Simbotin, and M. Gavrila, *ibid.* **82**, 665 (1999).